New Equipment for Measurement of Soiling and Specular Reflectance on Solar Mirrors

Estelle Le Baron, Antoine Grosjean, Delphine Bourdon, Anne-Claire Pescheux, Angela Disdier, Frédéric Vidal

New Equipment for Measurement of Soiling and Specular Reflectance on Solar Mirrors

Estelle Le Baron[1, a)], Antoine Grosjean[1], Delphine Bourdon[1], Anne-Claire Pescheux[1], Frédéric Vidal[1], Angela Disdier[1]

[1]*Univ. Grenoble Alpes, CEA-LITEN, INES, 50 avenue du Lac Léman, F-73375 Le Bourget du Lac, France*

[a)] Corresponding author: estelle.lebaron@cea.fr

Abstract. During the life time of Concentrated Solar Power (CSP) plants, optical performance of solar mirrors is affected by soiling phenomena and surface degradation. It is imperative to dissociate soiling that requires cleaning from irreversible degradations which affect the plant performance. In both cases, small degradations or dust deposition cause an optical reflectance loss. In order to provide an adequate cleaning strategy, operators need to determine soiling-induced performance loss. Several commercial instruments already exist to measure optical reflectance, but they are dedicated to a single wavelength range or angle, punctual measurements or to laboratory analyses. CEA has developed a new kind of laboratory sensor to measure separately the loss of reflectance due to the degradation and soiling, thanks to a CCD camera and photodiodes. This equipment allows addressing variable wavelength, incidence and acceptance angles, to compare specular and hemispherical reflectance from other devices. The analysis of the images will quantify the soiling rate in order to optimize the frequency of cleaning water operations. The aim of the present contribution is to distinguish soiling from degradations (abrasion or corrosion of the reflective layer). This paper reviews the different current research works on prototype instruments and a comparison of this new alternative instrument with available commercial ones.

INTRODUCTION

Concentrated Solar Power (CSP) technologies concentrate solar radiation by means of mirrors onto a thermal absorber where it is collected and converted to thermal energy. For scientists or for plant operators, it is necessary to evaluate solar field performance by measuring the quantity of sunbeam enable to reach the thermal absorber. Measurement of the solar reflectance, the capacity to a mirror to reflect radiative solar power, is studied in the SolarPACES task III to improve the current Reflectance Guideline [1].

The most relevant parameter to properly characterize solar reflectance from mirrors is the solar-weighted specular reflectance [1]. The specular reflectance describes the case where all the incident light at an angle θ_i [°] is reflected at an angle θ_r [°] measured at any distance from the boundary with a certain amount of scattering. The measured spectral specular reflectance for solar applications is written $\rho_{\lambda,\varphi}(\lambda,\theta_i,\varphi)$ where $\rho_{\lambda,\varphi}$ is dependent on the wavelength λ [nm] and is function of the incidence angle θ_i, as well as the half acceptance angle φ [mrad] or acceptance angle 2φ [mrad], associated with the detector aperture.

Actually, the spectral specular reflectance measurement for variable angles is not evident, due to the difficulty to have an instrument of characterization in the solar spectral wavelength range, for a reasonable cost, a high-resolution accuracy and an operating speed. Moreover, the theoretical measurement must operate in the solar spectrum domain from 280 to 2500 nm [3] and for a large panel of incidence angles. For these reasons, the development of new laboratory prototypes is being supported in the SolarPACES task III by several research institutes : “Solar mirror Qualification” (SMQ) by ENEA [3, 4], “Spectral Specular Reflectometer” (S2R) by DLR [6], “Very-Low Angle Beam Spread” (VLABS) by FRAUNHOFER-ISE [7- 9] and a custom spectrophotometer by the University of Zaragoza. A summary of these new specular reflectometer prototypes is presented in TABLE 1 [10].

TABLE 1. Comparison between new reflectometer prototypes

Instruments	Reflectance	wavelenght	Incidence Angle θ_i	Half acceptance Angle φ
SMQ2 (ENEA) [3,4]	Near-specular	485; 530; 640 nm	3°	3-50 mrad
VLABS (Fraunhofer ISE) [7, 8, 9]	Near-specular / Sun-conic	450; 550; 600; 650 nm	10°-70°	1-33 mrad
S2R (DLR/CIEMAT) [6]	Sun-conic	320-2500 nm	10°-70°	9.8-107.4 mrad
Custom spectrophotometer (University of Zaragoza)	Sun-conic	320-2500 nm	10°	15 mrad

Other devices are actually available on the market as the pFlex by Fraunhofer ISE, the Condor reflectometer by Abengoa, the 15R-USB reflectometer by D&S and the TRACS system by DLR. The first three sensors are portable and manual reflectometers limited to a single wavelength at near-normal incidence angle and dedicated to make direct measurements on CSP plants, while the last one is immovable and previously measures a reference mirror with near normal incidence angles. Nevertheless, for CSP applications, incidence angles up to 50° or even more are relevant and should be part of the optical analysis. The commonly employed equipment are currently not able to fully characterize the mirrors with the incidence and acceptance angles of a CSP plant [11]. Furthermore, the ideal equipment must be able to characterize a clean or soiled mirror without contaminate itself. Soiling on a mirror is a major problem in optical characterization because soiled samples risk to contaminate the measurement equipment and its optical components. They are most of the time prohibited in laboratories with costly equipments.

This paper goal is to present and evaluate a new soiling reflectance equipment patented in our laboratory [12]. To overcome the drawbacks of commercial instruments, this new equipment is able to scan a large panel of incidence and reflected angles (from 15° to 65°) with various wavelengths (365-850 nm) covering the solar spectra. It allows to observe the surface of several mirror samples by a CCD camera, count the particles on the surface and determinate several additional information as to their shape, their size distribution and the percentage of covered area. This method is without contact, gives rapid results and causes no degradation on the sample.

DEVELOPMENT OF A SOILING REFLECTANCE PROTOTYPE

Design of the Soiling Sensor Prototype Equipment

The prototype is shown in FIGURE 1. The light source is deported and produced by a LED system (-1- in FIGURE 1(a)) and injected through an optical fiber of 1 mm diameter to the light emission head (-2- in FIGURE 1(a)). As to ensure the light emission on the mirror, a first lens collimates light, and a second one is focused on the mirror. The focal value has been set at 100. The reception head (-3- in FIGURE 1(a)) and the emission head are set on a circular rail, and the angular position is automatized with a motor (in green in FIGURE 1(b)) The mirror is observed with a CCD camera (reception head -3-FIGURE 1(a)), but the lightened area is then quite much larger (f' = 50 mm) , with of course a lightening at lower intensity. A separating blade is added on the optical emission and reception paths, before the second lens, in order to send a part of the light beam on a photodiode (in blue in FIGURE 1(b)). This is giving information on the light beam intensity and is used for reflectance measurements. On the reception head, the focal of the collection lens (at 100 mm) is associated to a lens with a 25.4 mm diameter. It so gives an aperture angle at about 40 mrad (2.3°). The actual CCD camera from ThorLabs is able to take black and white pictures in grey level with a resolution of 1024 x 768 pixels and enables the particle detection by image processing.

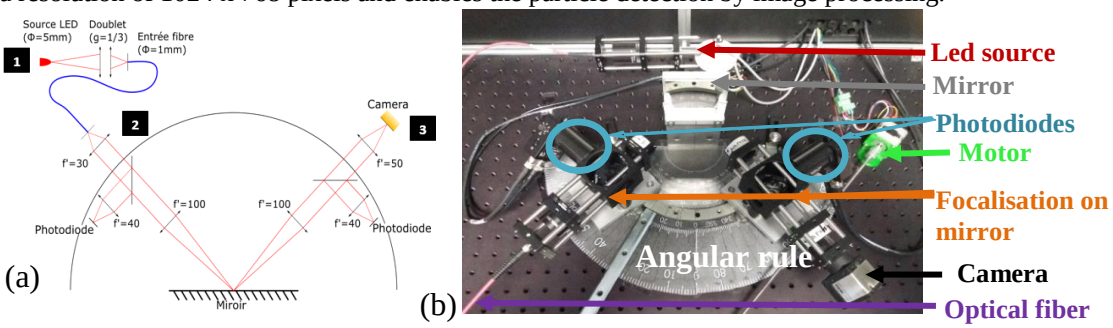

FIGURE 1. (a) Optical principle scheme and (b) picture of the sensor prototype

To avoid parasitic reflectance with light in the measurement room, a 890 x 583 x 223 mm^3 light-tight box encloses the lab bench. This device allows the observation of the mirror surface and so the defaults located on the surface (FIGURE 2). On a perfect surface, a uniform white lightening is observed, while degradations and soiling appear as area with a reduced light intensity.

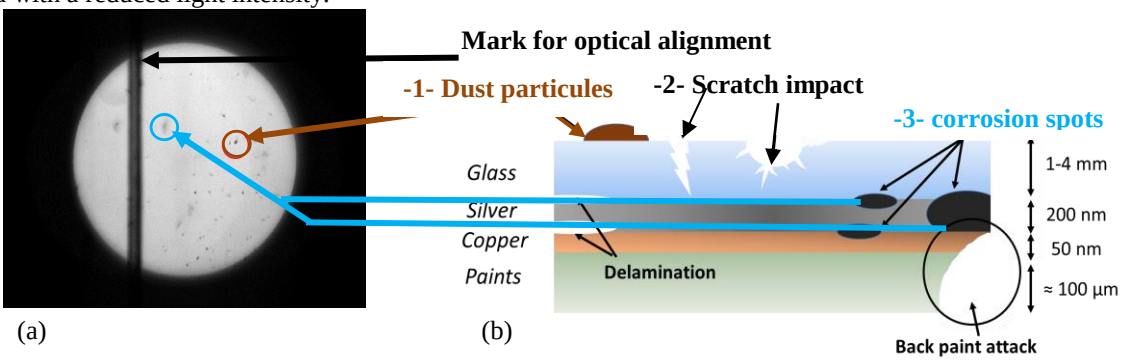

FIGURE 2. Observation of the glass mirror surface with a focused lightening: (a) picture taken by the CCD camera, (b) schematic representation of the different located defaults

Soiling particles (-1- in FIGURE 2 (b)) appear as small sharp circular net black spots and are distinguished from erosion larger (>100 µm) line-shaped (-2- in FIGURE 2 (b)) and from corrosion spots (-3- in FIGURE 2 (b)) on the silver reflecting coating (few millimeters away). These last ones appear in light gray with a less distinct outline because they are located at the back and observed as wide area. An image-processing is so expected to discriminate for a given measure, the number of soiling spots, the associated area and the number of scratches and corrosion area. Therefore, a level of soiling, corrosion and scratches is expected to be determined. The whole prototype is controlled thanks to an Arduino Uno piloted by a computer close to the optical device. This allows the selection of the light source and the angles studied, the recovery of the photodiodes, the calculation of the reflectivity ratio and the tracking of the images recorded by the camera. Finally, an image processing with a dedicated software presented below gives the total number of particles and their size distribution.

Specifications of the Soiling Sensor Equipment

The main characteristics of the actual new laboratory soiling sensor prototype are described below:

- Ten leds with a large wavelength range of 365-850 nm can be considered (common optics would have triggered chromatic issues). Even if this range is not wide enough to cover the whole solar spectra (280-2500 nm), it is considered as the widest of developed and commercial products.
- Range of incidence and reflectance angles between 15° and 65°
- Automatic control of the incidence and reflectance angles realized by motorized displacement
- Specular reflectance measuring a window of 3mm diameter for a mirror size from 10x10mm^2 to 100x100mm^2
- Acceptance angle for reflectance measurement of 2φ = 40 mrad

Calibration of the Soiling Sensor Equipment

The first test performed with the soiling sensor prototype aimed to the qualification of the photodiodes at each incidence angle. The test has been realized only with a 660 nm wavelength led on two similar mirrors: one new (solid lines) and one degraded and soiled (dashed lines). Firstly, the parasitic noises received by the photodiodes from the environment are subtracted. Secondly, we compared the signal received from degraded and soiled mirror samples (dashed lines). This one is reduced at about 20% compared to brand new ones (solid lines). This obvious result confirms that the reflected signal is function of the sample quality. Finally, for a same sample (solid line or dashed line), the maximum of reflected signal is function of the incidence angle, which is maximum at 25°on the FIGURE 3 and continuously decreases with increasing angles.

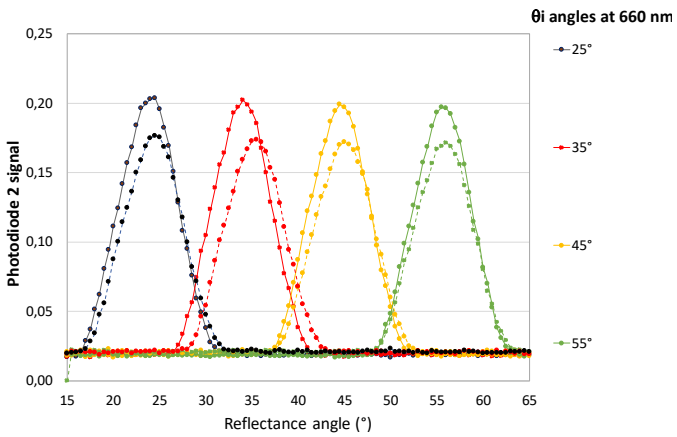

FIGURE 3. Measurements of photodiode 2 signals for cleaned or referency new mirror (solid lines) and for degraded mirrors (dotted lines) for several incidence angles

As a commercial reflectance measurement instrument, this soiling sensor prototype requires a reference mirror for its calibration to perform absolute specular measurements. The signal received by the photodiode 2 enables the reflectance measurement and allows the comparison with the value received by a reference mirror with a known reflectance. The intensity of the signal received by the photodiode is set as reference. The absolute reflectance value of the reference mirror is based on the value obtained thanks to the specular reflectometer D&S 15R-USB [13], with a light-emitting diode source of $\lambda = 660$ nm, at an incidence angle $\theta_i = 15°$ and an half acceptance half angle $\varphi = 12.5$ mrad. The raw signals of the photodiodes are processed to calculate the reflection factor with a correction coefficient from the calibrated mirror and the offset of the background noise of the photodiodes. The system is calibrated at an incidence angle of 15° with the D&S and the known value of the reference same mirror, and it does not need recalibration with other angles and same manufacturer mirrors.

RESULTS

Sample Presentation

Silvered glass reflectors are widely used in CSP plants. Therefore, the three samples types selected in this study are three second surface monolithic silvered glass mirror samples provided by commercial manufacturers, anonymized in this paper and noted #1 to #3. Each manufacturer sample has different glass thicknesses (respectively 1 mm for #1, 3 mm for #2 and 4 mm for #3). The sample size is 70 mm x 70 mm. This size is used in our laboratory for ageing tests and allows to compare edges and center ageing mechanics. For each manufacturer, one mirror has been kept intact (without exposure) as references. Various soiling and aged states are studied to qualify the sensor prototype as detailed in the next tables. Each sample is noted according to his manufacturer number (#1 to #3) followed by another number (see TABLE 2). Samples 1-1, 2-1 and 3-1 from manufacturers #1, #2, #3 are the reference mirrors without ageing. The second mirror 1-2 has been exposed to an erosion test in a sandblasting chamber with normalized sand MIL-STD 810-F. This sample shows very high damages, with a high number of micrometric white points on the mirror surface. Each point is an impact of sand particles on the glass. Sample 1-3 and 1-4 have been exposed outside with different soiling rates during summer 2017 at INES, Le Bourget du Lac, France. Sample 1-3 has been exposed during one week and sample 1-4 during three weeks, without rain events in both cases. Samples from manufacturer #2 and #3 have been indoor accelerated aged in thermal and irradiation chambers, according to several accelerated thermal and UV ageing tests [14, 15]. We have chosen various heterogeneous samples and ageing tests in order to have very varied measurements to achieve the qualification of the new soiling reflectance equipment.

Samples from manufacturers #2 and #3 also include: the sample 2-1and 3-1 as reference mirrors, the sample 2-2 exposed to a constant temperature of 70°C during a 20820 h artificial ageing and the sample 2-3 exposed to a constant temperature of 100°C during 8000 hours. The sample 3-2 exposed to 130°C for a 1000 hours artificial ageing, as the sample 2-3. We can observe a visible impact of the high temperature on the reflective layer. The sample 3-3 has been submitted to high UV flux density (200 W/m^2, ≈ 5 times the natural UV flux density according to ASTM G173-03 DC) for 2303 hours on the front-side of the reflective surface.

TABLE 2. Samples codes and aging tests of manufacturers #1, #2 & #3

Samples Type #1	**Reference t = 0 h**	**Abrasive test with sand**	**Natural soiled Low dust level / high dust level**	
	1-1	1-2	1-3	1-4
Type #1		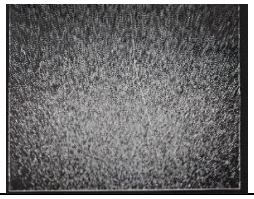		
Samples Type #2	**Reference t = 0 h**	**T°C= 70°C, t = 20820 h**	**T°C=100°C, t = 8000h**	
	2-1	2-2	2-3	
Type #2	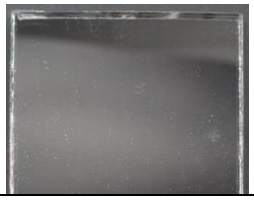			
Samples Type #3	**Reference t = 0 h**	**T°C= 130°C, t = 1000 h**	**UV: 200 W/m2, t = 2303 h**	
	3-1	3-2	3-3	
Type #3	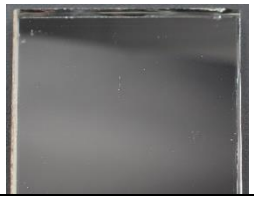		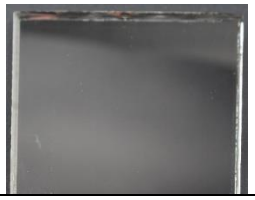	

Optical Characterization

Our laboratory decided to make a comparison of reflectance measurement equipments on three types of mirrors, presented in the previous paragraph. The testing campaign comparison is performed to validate the performances of the laboratory soiling sensor with various commercial equipments :

TABLE 3. Overview of reflectance instruments and methods used in this study

Instrument	**Manufacturer**	**Model**	**Reflectance**	**Incidence Angle θ_i**	**Acceptance Angle 2φ**
Reflectometer	D&S	15R-USB [13]	Specular reflectance $\rho_{\lambda,\varphi}$(660nm,15°,12.5mrad)	15°	25 mrad
Spectrophotometer	Perkin Elmer	Lambda 950 ARTA [16]	Specular reflectance $\rho_{\lambda,\varphi}$(660nm,θi, 262mrad) Specular spectral reflectance $\rho_{s,\varphi}$ ([280-2500],θi,262mrad)	8°/45°/65°	262 mrad / 58 mrad
Spectrophotometer	Perkin Elmer	Lambda 950 Integrating sphere (Ø 150 mm) [17]	Hemispherical reflectance $\rho_{\lambda,h}$(660 nm, 8°,h) $\rho_{s,h}$([280-2500],8°,h)	8°	-
Soiling sensor prototype	CEA		Specular reflectance $\rho_{\lambda,\varphi}$(660nm, ,θi, mrad)	15°/45°/65°	40 mrad

The ARTA and the soiling sensor prototype are designed to characterize the angular scattering of mirrors before and after degradation or soiling at different angles. Solar-weighted specular and hemispherical reflectance, $\rho_{s,\varphi}$ ([280-2500], θ_i, 262mrad) and $\rho_{s,h}$([280-2500], 8°, h) are calculated following the weighting formula described in [18] using the direct normal Air Mass 1.5 ASTM G173-03 standard spectral irradiance distribution. The wavelength range which

allows accurate solar weighted calculation is fixed at λ = [320-2500] nm in the Reflectance Guideline [1], but we use the wavelength range 280-2500 nm for UV considering the hemispherical and specular reflectance spectrophotometer measurement. It is also recommended in [1] to measure at several (at least three) narrow wavelengths (line width similar to that of hemispherical measurements) appropriately spaced along the solar spectrum or at a specified wavelength range that accounts for differing wavelength dependent scattering properties.

Specular and Hemispherical Reflectance Results

In this section, we discuss of the various results obtained with the soiling equipment prototype and the actual device used to perform similar reflectance analysis.

At Incidence Angles $\theta_i \leq 15°$: Comparison of Equipments

Reflectance values are measured with the D&S, the Perkin Elmer spectrophotometer Lambda 950 with ARTA and IS commercial devices, and with the soiling sensor prototype, for each sample at 660 nm and low incidence angles ($\theta i \leq 15°$). TABLE 4 gives the average reflectance (in percentage) for each sample with the four equipments. We recall that the reflectance value of sample 1-1 obtained with specular reflectometer D&S 15R-USB is exactly the same that the one obtained with the soiling sensor. The soiling equipment prototype shows a good correlation with the actual equipment. The results obtained here present a good homogeneity with the other results. We only note two exceptions: for sample 1-2 and sample 3-3. For sample 1-2 (mirror with sand particle impacts), our prototype gives similar results as Lambda 950 with ARTA device (38.8% vs 37.7%) when D&S and IS give more dispersed results (respectively 22.9% and 87.4%). The sand particle impact on the glass created a more diffused surface (see in TABLE 2). If the specular reflectance quickly decreases, the total diffused reflectance is similar, which explain the results gave by the Lambda 950 with IS. The small size of the spot makes the measurement with the D&S very variable depending on the light point on the glass contact surface. For samples with natural soiling (1-3 and 1-4), the results are similar to the ones obtained with the portable device (D&S). The standard derivation with the soiling equipment is 2% compared to the actual equipment (error of 2% on spectrophotometers integrating-sphere measurements [19]).

TABLE 4. Reflectance at 660 nm of each sample with the four equipments with highlighted minimal and maximal values (red : 1-1, green : 1-2, blue : 1-3, black : 1-4)

Samples	1-1	1-2	1-3	1-4	2-1	2-2	2-3	3-1	3-2	3-3
D&S	**96.5 %**	**22.9 %**	**90.5 %**	82.7 %	96.3 %	94.1 %	86.1 %	95.7 %	80.2 %	93.9 %
Soiling sensor	**96.5 %**	38.8 %	91.1 %	**81.7 %**	96.4 %	93.7 %	84.1 %	95.9 %	80.9 %	90.2 %
Lambda950 ARTA	96.1 %	37.7 %	92.9 %	82.5 %	95.8 %	93.5 %	85.0 %	95.1 %	79.7 %	93.2 %
Lambda 950 IS	96.3 %	**87.4 %**	**95.4 %**	**86.7 %**	96.2 %	93.9 %	88.4 %	95.6 %	85.2 %	94.1 %

At this point, we can conclude that this soiling equipment can perform a similar role as the D&S, but with various angles and the possibility to take pictures of the sample (see next section). The large spot size gives more replicated results than D&S, especially on the mirror with sand impacts. However, the equipment offers the possibility to perform measurements of soiling sample without the risk to contaminate the device with a notifiable accuracy.

At Incidence Angles $\theta_i \leq 15°$: Effect of Dust and Degradation

Dust and sand particles lead to additional absorption and scattering that can not be measured with specular reflectance $\rho_{\lambda,\varphi}$ commercialized instruments like ARTA and D&S. It also depends on the choice of the half acceptance angle φ. The amount of diffraction and/or scattering radiation is influenced by the particle morphology (size, shape, chemical composition …). CEA made a study to compare the spectra acquired with the same spectrometer (Lambda 950 from Perkin Elmer) with two different accessories, an integrating sphere of 150 mm diameter and the specular ARTA module. With the ARTA module, the first incidence angle chosen was 8°, the same as the integrating sphere. The results presented here are the curves of the thin mirrors from manufacturer #1. Spectra and Solar-weighted specular and hemispherical reflectance results are identical for cleaned and low degraded mirrors, discrepancies are less than 0.5% : $\rho_{s,\varphi}([\lambda_a\text{-}\lambda_b],\theta_i,\varphi) \sim \rho_{s,h}([\lambda_a\text{-}\lambda_b],\theta_i,h)$ but not when the mirror is degraded or soiled (typically samples 1-2 and 1-4). The specular reflectance loss related to degradation by abrasion with sand wind artificially simulated on

the mirror 1-2 is constant over the entire solar spectrum (see FIGURE 4) whereas hemispherical reflectance is higher. These differences determine the amount of energy lost due to scattering of the mirror 1-2. Conversely, soiling particles preferentially decrease the UV/VIS wavelength (< 1000 nm). The reason is an increase of the scattered reflectance outside the specular direction. This is due to the front surface degradation undergone by the reflector, which is detected by the ARTA (φ = 262 mrad), the D&S (φ = 12.5 mrad) and the soiling sensor prototype but not by the integrating sphere. Dust particles lead to additional absorption and scattering.

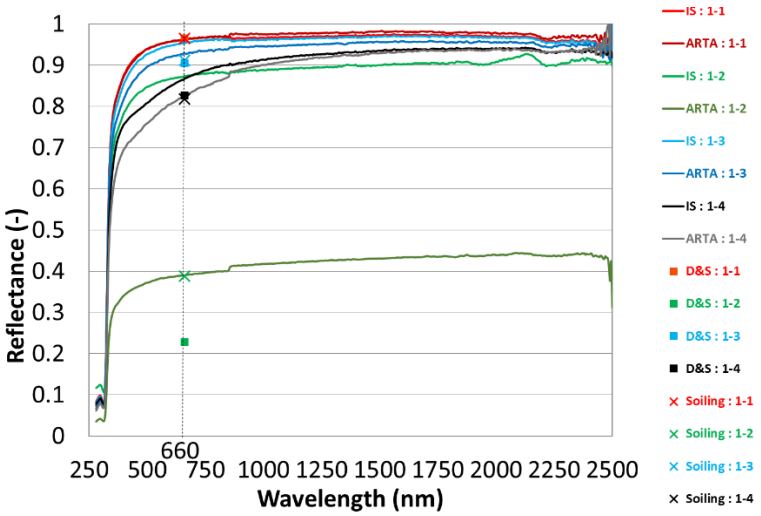

FIGURE 4. Spectral reflectance values of four silvered glass mirror samples from manufacturer #1 θi ≤15° with the four equipment with the sample color code : red 1-1, green 1-2, blue 1-3, black 1-4

These results are also obtained for the very specular mirrors, manufacturers #2 & #3, such as silvered glass (3 and 4 mm thick), present similar spectra for hemispheric and specular reflectance.

At Incidence Angles θ_i >15° : Reduced Acceptance Angle and Increasing Angles Effects

Hemispherical spectral reflectance measurement is performed only at near-normal incidence 8° with a spectrophotometer combined with an integrating sphere. As well, it is possible to measure reflectance at λ= 660 nm and θ_i =15° with the portable reflectometer 15R-USB from D&S. Only the ARTA accessory with the spectrophotometer Lambda 950 of Perkin Elmer allows rotating angle for various reflectance measurement. The soiling sensor prototype reflectance measurement is then compared in this section to the variable angle ARTA specular directional reflectance results at θ_i =45°. For example, FIGURE 5 shows comparative results between the specular reflectance at a wavelength of 660 nm and 45° of incidence angles measured by the two equipment for the silvered glass mirrors type #1.

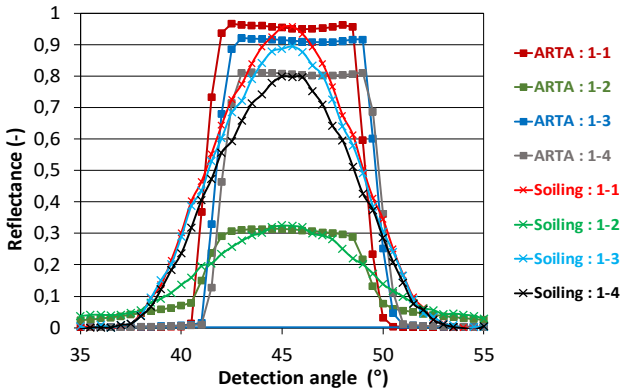

FIGURE 5. Comparison of specular reflectance values measured with the ARTA module (φ = 262 mrad) and the soiling sensor prototype (φ = 40 mrad), for 4 silvered glass mirrors type #1, at θ_i = 45° and various detection angles

FIGURE 5 shows the ability to measure the absolute reflectance distribution and the reduced acceptance angle of the soiling sensor prototype increases the measurement resolution of the angular spread from the ARTA tool. As it can be observed in FIGURE 5, the reflectance measurements for the mirrors type #1 are very similar for low incidence angles with a maximum difference of 0.016 for sample 1-1 and of 0.025 for the mirrors sample 1-3. The differency are largely for higher incidence angles (θ_i). It could be due to differency in acceptance angle (2φ) from ARTA (262 mrad) and the soiling sensor prototype (40 mrad). The ARTA acceptance angle could be reduced to 58 mrad by varying the detector aperture for specular materials such as mirrors. The four pictures on FIGURE 6 are taken by the CCD camera.

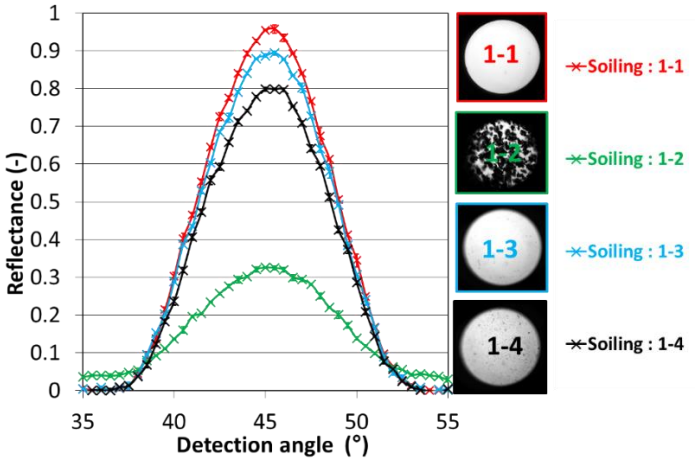

FIGURE 6. Reflectance values of four silvered glass mirrors type #1 and camera spots of the eroded (sand > 100 µm) and soiled mirrors (local continental dust)

As shown in FIGURE 6, this first soiling sensor prototype has shown good results in terms of angular resolution measurements (0.5°) and repeatability along time. As it can be observed in FIGURE 6, the reflectance measurements for the silvered-glass reflectors are very similar, with an average standard deviation of ±0.004 and a maximum standard deviation of ±0.02 for an incidence angle θ_i of 45°. An important improvement for the ARTA module and the soiling sensor prototype compared to the other instruments is the possibility to measure various incidence angles (not only the near normal reflectance) with a good resolution. With incidence angle θ_i increasing from 15° to 65°, the specular reflectance of the soiling sensor prototype decreases with the increasing angle from 5% for referency and soiled mirrors to 32 % for eroded one due to scattering effects more visible at elevated angles. The commonly employed equipment are currently not able to study the influence of incident angles in the overall efficiency of the solar collector. Similar results are obtained with the mirrors type #2 and type #3.

Images Treatment

The main advantage of our soiling sensor prototype compared to the tested commercial equipment (see TABLE 3) is the presence of a CCD camera, which allows a complementary analysis by taking pictures of the sample surface, especially in near normal incidence for avoid deformation due to the perspective. The advantage provided by the CCD camera is double.

- Firstly, the operator can have a direct observation of the sample surface. By moving the sample, he can choose where to focus the reflectance measurement. By this way he can look for a specific area on the sample with impacts, damages, scratches, different soiling levels or just a clean area. Visual analysis of the sample can give additional information compared to standard measurements (D&S, ARTA or IS).
- Secondly, image processing is possible. Actually, the image treatment is performed on Scilab (5.5.2) with the Image Processing Design (IPD) toolbox (8.8.3) [20]. In the near future, we have planned to upgrade the image treatment thanks to deep learning or artificial neural network analysis [21]. By this way, we plan to identify automatically the soiling level and the potential presence of impacts, damages or scratches. For performing an efficiency deep learning, we need a huge database with thousand of examples, actually under construction.

During the image acquisition, the software calculates the exposure time and the captor sensitivity using the "exposing to the right" technique, also called ETTR. As each B&W pixel is coded with an integer value from 0 (pure black) to 255 (pure white), the aim is to obtain a histogram (the pixel values distribution) included between 1 and 254. By this way, no information is destroyed by a picture area too dark or too bright. Secondly, each image captured by the camera is corrected with a dark picture and a bright picture for noise reducing and remove the potential dust on the CCD captor. In some cases, as very damage samples, an additional brightness correction for increase the contrast is necessary. Finally, any objects on the mirror are detected using a method of edge detection filters.

Each object detected appears as pure white pixels when surface sample appears as pure black pixels. We present in FIGURE 7, the different results obtained with manufacturer #1. The same results and same conclusion can be obtained with manufacturers #2 and #3. Overall, the image treatment method shows good results: the total area covered by objects detected is direct a function of the reflectance loss measurement (D&S or ARTA). As expected, sample 1-1 (the reference mirror) shows only one object when sample 1-4 (highest dust level) shows several objects. For sample 1-2 (sand mirror) the results obtained are a function of the reflectance and of the impact density. The differentiation between impact and no-impact areas performed well but error can be committed. In an area with several impacts (as shown here), the impact overlap makes confused the treatment of the image (top left corner).

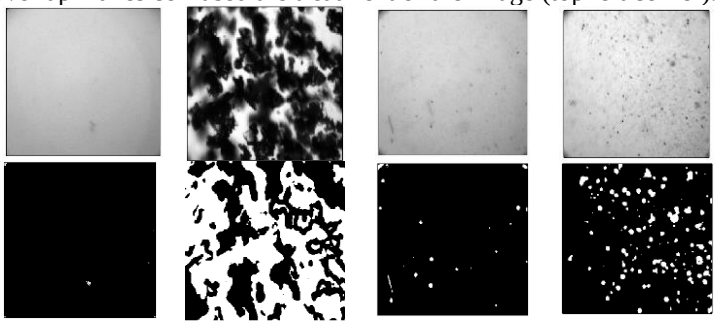

FIGURE 7. Above : B&W pictures of the samples from the CCD camera. Below : particles detected (pure white) on sample (pure black) using edge detection

It is also possible to analyze the shape and the size distribution of the particles present in the sample. The particles are express according to their pixel size, by an edge-to-edge method. FIGURE 8 gives a good example of the possibility, illustrated here by the samples 1-1 to 1-4. As expected, sample 1-3 and sample 1-4 (mirrors exposed outside at two different levels of soiling) have the highest level of particles detected. For the entire samples presented, the size distribution is very similar, only the total number has changed. Each particle detected is surrounded by a red square on the mirror's pictures available in FIGURE 8. Reference mirror (sample 1-1) has naturally the lowest level with nine particles, which are a mix of real particles on the mirror and few particles on the CCD camera. Despite of the very damage area, sample 1-2 (sand test mirror) has also a low level of particles detected: the impact of sand particles are not confused with the smallest particles. Furthermore, this method allows classifying easily the soiling level on solar mirrors.

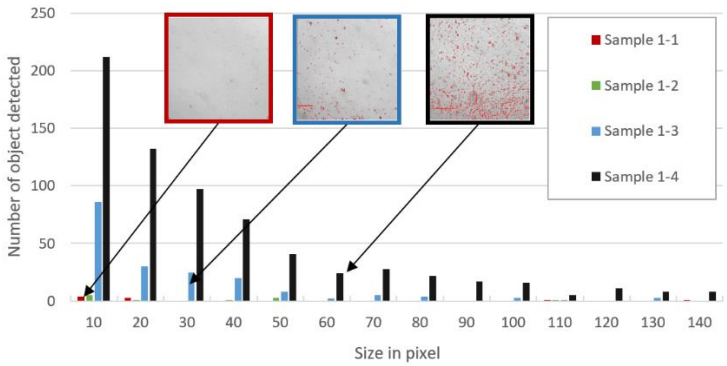

FIGURE 8. Number of soiling particles detected according to their size in pixel on samples 1-1 to 1-4

DISCUSSIONS AND FUTURE WORK

The specular reflectance is noticeably lower than the hemispherical one for dusty and damaged silvered glass mirrors. Dust and sand particles lead to additional absorption and scattering. Whereas the degradation affects all the solar spectra wavelengths, the soiling and dust particles affect the range 280–1000 nm spectral wavelengths of the total reflectance of the mirror materials (Figure 6). The new soiling sensor shows a good correlation with D&S and ARTA equipment for directional reflectance results. With the variable angle specular equipment (soiling/ARTA), the most prominent result of these measurements is a reduced acceptance angle of the soiling sensor prototype from ARTA that improves the measurement distribution of the angular spread (Figure 7). Another important result is that the reflectance decreases significantly while the angle of incidence increases (Figure 9). The directional specular reflectance results of multiple reflectors are nearly equal between the soiling sensor prototype and the ARTA equipment.

The presence of the CCD camera makes simultaneously possible digital images processing. The first step performed here, with a simple edge detection is able to detect objects on the sample and classified different levels of dust. The area covered by the objects can be linked to the specular reflectance measurement. We can also use similar tool to identify corrosion spots and calculate damaged area of mirror. However, it is not actually possible to classified objects as impacts, damages, scratches or dust particles, with the algorithm used with a low error risk. This work is actually performed by a human operator. Deep learning or artificial neural network analysis can do this task. These two methods require an important data bank of pictures, not available yet but in progress for future development. Another prospect of this study will be to use several LEDs covering a large part of the solar spectrum to quantify more precisely the level of soiling. Moreover, an automation of the prototype would allow a better precision, reproducibility and speed of measurements.

The experimental study is limited to low number of soiled and degraded samples and need further aging and natural sites exposure conditions. Also in future research, the study will also include measurements with the portable soiling sensor developed by OMT to evaluate the detectability of soiling, scratching and other forms of degradation by imaging the mirror surface at normal incidence.

CONCLUSION

This paper discusses in details the reflectance results of various devices on different solar silvered glass mirrors. The main goal of this study is to present the first results of a new test bench and to compare the values obtained using the 660 nm single-wavelength optical bench with those of commercial devices. The soiling sensor prototype shows similar absolute reflectance results as all the commercialized ones. Furthermore, the large area covered by the LED spot on the sample allows the soiling sensor prototype to give a more representative reflectance value, similar to the one obtained with heavy equipment, like spectrophotometer with ARTA device.

The taking of simultaneous pictures from different angles of view with digital images processing allows analyzing the number and the size distribution of the particles deposited on the sample surface.

The two main advantages of this prototype compared to the existing devices are:

- The ability to measure quickly and precisely the absolute reflectance distribution over a large range of incident and detection angles (15° to 65°), a reduced acceptance angle that increases the measurement resolution of the angular spread and a simultaneous image taking that allows a complementary analysis (especially in grazing light).
- The ability to distinguish the level of soiling from irreversible damages on the mirror without the risk to contaminate the equipment (no contact between the sample and the optical device).

ACKNOWLEDGEMENT

The authors would like to acknowledge the European Union through the H2020 research and innovation program for the financial support of this work in the WASCOP project under grant agreement No. 654479.

REFERENCES

1. A. Fernandez-Garcia and al., “Parameters and method to evaluate the reflectance properties of reflector materials for concentrating solar power technology, V 3.0” (2018).
2. A. Fernandez-Garcia and al., “Simplified analysis of solar weighted specular reflectance for mirrors with high specularity”, in Proceedings of the AIP Conference 1734, 2016.
3. A. Fernandez-Garcia and al., “Equipment and methods for measuring reflectance of concentrating solar reflector materials”, Sol. Energy Mater. Sol. Cells 167 (2017), pp. 28–52.
4. M. Montecchi, “Approximated method for modelling hemispherical reflectance and evaluating near-specular reflectance of CSP mirrors”, Sol. Energy 92 (2013), pp. 280–288.
5. M. Montecchi, “Upgrading of ENEA Solar Mirror Qualification Set-up”, Energy Procedia 49 (2014), pp. 2154-2161.
6. F. Sutter and al., “Spectral characterization of specular reflectance of solar mirrors”, Sol. Energy Mater. Sol. Cells 145 (2016), pp. 248–254.
7. A. Heimsath and al., “Detailed optical characterization of reflector materials for CSP applications”, SolarPACES Conference 2010.
8. A. Heimsath and al., “Angle resolved specular reflectance measured with VLABS”, Energy Procedia 69 (2015), pp. 1895–1899.
9. A. Heimsath and al., “Specular reflectance of soiled glass mirrors – Study on the impact of incidence angles”, SolarPACES 2015.
10. F. Sutter and al., “Advanced Measurement Techniques to Characterize the Near-Specular Reflectance of Solar Mirrors”, SolarPACES Conference 2018.
11. F. Sutter and al., “The effect of incidence angle on the reflectance of solar mirrors”, Solar Energy Materials and Solar Cells 176 (2018), pp. 119-133.
12. Patent EN 17 61041 O. Raccurt and al., “Système de surveillance de la dégradation et de l'encrassement d'un miroir", CEA.
13. Devices and Services Company, Devices and Services Portable Reflectometer Model 15R- USB .
14. C. Avenel and al., “Accelerated aging test of solar mirrors: Comparison of different UV chambers”, SolarPACES Conference 2017.
15. C. Avenel and al., “Review of accelerated aging test modeling and its application to solar mirrors, Solar Energy Materials and Solar Cells”, Volume 186, November 2018, pp. 29–41.
16. OMT Solutions BV, ARTA – Technical Description, 2010.
17. Sphere Optics. Integrating Sphere Design and Applications. Technical information. Sphere Optics, 2007.
18. ASTM G 173-03, Terrestrial Reference Spectra for Photovoltaic Performance Evaluation, ASTM, 2012.
19. D.I. Milburn and K.G.T. Hollands, “The directional response error in integrating-sphere transmittance measurements at solar wavelengths”, Solar Energy, Volume 55, August 1995, pp. 85-91.
20. Harald Galda, “Image processing with Scilab and Image processing Design Toolbox Copyright”, 2011.
21. Priyadarshni and J.S. Sohal, “Improvement of artificial neural network based character recognition system, using SciLab”, Optik, Volume 127, Issue 22, 2016, pp.10510-10518.